Front. Earth Sci. 2023, 17(4): 997–1011
https://doi.org/10.1007/s11707-022-1082-2

RESEARCH ARTICLE

Late Holocene brGDGTs-based quantitative paleotemperature reconstruction from lacustrine sediments on the western Tibetan Plateau

Xiumei LI[1], Sutao LIU[1], Juzhi HOU (✉)[2], Zhe SUN[3], Mingda WANG[4], Xiaohuan HOU[2], Minghua LIU (✉)[1], Junhui YAN[1], Lifang ZHANG[1]

1 Henan Key Laboratory for Synergistic Prevention of Water and Soil Environmental Pollution, School of Geographic Sciences, Xinyang Normal University, Xinyang 464000, China
2 Institute of Tibetan Plateau Research, Chinese Academy of Sciences, Beijing 100101, China
3 Institute of Geography and Resources Science, Sichuan Normal University, Chengdu 610066, China
4 School of Geography, Liaoning Normal University, Dalian 116029, China

Abstract We present a quantitative mean annual air temperature (MAAT) record spanning the past 4700 years based on the analysis of branched glycerol dialkyl glycerol tetraethers (brGDGTs) from a sediment core from Xiada Co, an alpine lake on the western Tibetan Plateau (TP). The record indicates a relatively stable and warm MAAT until 2200 cal yr BP; subsequently, the MAAT decreased by ~4.4°C at ~2100 cal yr BP and maintained a cooling trend until the present day, with centennial-scale oscillations centered at ~800 cal yr BP, ~600 cal yr BP, and ~190–170 cal yr BP. MAAT decreased abruptly at ~500–300 cal yr BP and reached its minimum for the past 4700 years. We assessed the representativeness of our record by comparing it with 15 published paleotemperature records from the TP spanning the past ~5000 years. The results show divergent temperature variations, including a gradual cooling trend, a warming trend, and no clear trend. We suggest that these discrepancies could be caused by factors such as the seasonality of the temperature proxies, the length of the freezing season of the lakes, the choice of proxy-temperature calibrations, and chronological errors. Our results highlight the need for more high-quality paleotemperature reconstructions with unambiguous climatic significance, clear seasonality, site-specific calibration, and robust dating, to better understand the processes, trends, and mechanisms of Holocene temperature changes on the TP.

Keywords Tibetan Plateau, lake sediments, branched GDGTs, paleotemperature

Received October 31, 2022; accepted March 16, 2023

E-mails: houjz@itpcas.ac.cn (Juzhi HOU)
lmhhqs@126.com (Minghua LIU)

1 Introduction

Global warming has generated major concerns about the trend and amplitude of future temperature changes. While climate predictions rely mainly on climate models, quantitative paleotemperature reconstructions can help improve the accuracy of climate simulations by providing tests and evaluations of climate models (Snyder, 2010; Braconnot et al., 2012). The late Holocene is a critical period in the Earth's climate history because of the transition from forcing solely by natural factors to the additional forcing of anthropogenic greenhouse gases (IPCC, 2013). Quantitative reconstructions of temperature changes for the late Holocene are crucial for assessing the significance of recent anthropogenic warming within the context of natural climate variability (Feng et al., 2019; Yao et al., 2019; Li et al., 2023a).

Currently, the rate of temperature increase at high-elevation sites is much higher than the global average (Bradley et al., 2006; Mountain Research Initiative EDW Working Group, 2015). The Tibetan Plateau (TP), covering 2.5 million km^2 and with an average elevation of > 4000 m, is the largest high-elevation region on the Earth and is especially sensitive to global environmental changes (Yao et al., 2012, 2019; Li et al., 2021a). Observation data from meteorological stations on the TP indicate surface warming at a rate twice that observed globally (Chen et al., 2015). The TP is often referred to as 'Asia's Water Tower', as it hosts numerous mountain glaciers that provide an indirect water supply for hundreds of millions of people throughout Asia (Immerzeel et al., 2010). Over the last few decades, glaciers on the TP have experienced rapid and pronounced changes (Yao et al.,

2019), and there are increasing concerns about the potential effects on the hydrology, ecosystems, and human population of this region and elsewhere. The retreat and advance of the TP glaciers are closely related to temperature variations (Bolch et al., 2012; Jacob et al., 2012); hence, knowledge of paleotemperature variations on the TP can provide a valuable context for assessing the current and possible future status of its glaciers.

There are numerous paleotemperature reconstructions since the last deglaciation for the TP and the adjacent areas (Wang et al., 2015a; Hou et al., 2016; Li et al., 2017; Zhang et al., 2017; He et al., 2020; Zhao et al., 2021; Sun et al., 2022; Zhang et al., 2022). These records generally indicate a cooling trend of summer temperatures during the Holocene, although the patterns of mean annual temperature (MAAT) change on the TP remain controversial (Chen et al., 2020; Sun et al., 2022). In particular, MAAT reconstructions across the TP during the middle to late Holocene have yielded conflicting results. Several of these MAAT reconstructions show a cooling trend since the middle Holocene (Zhao et al., 2021), while others reveal a warming trend (Thompson et al., 1997; Li et al., 2017; Sun et al., 2022; Zhang et al., 2022). The mechanism responsible for these different temperature trends remains unclear. Hence, more quantitative MAAT reconstruction across the TP are needed to better understand the Holocene temperature dynamics of this region.

Branched GDGTs (brGDGTs) are increasingly regarded as a promising tool for continental climate reconstruction (Weijers et al., 2007; Li et al., 2023b). brGDGTs are membrane lipids synthesized by heterotrophic bacteria that contain two C_{28} alkyl chains with 4–6 methyl substituents and 0–2 cyclopenthy moieties, and they are ubiquitous within a wide range of terrestrial depositional environments (Weijers et al., 2006; Schouten et al., 2013). The brGDGTs-producing bacteria can alter the fluidity of the lipid membrane, enabling it to adapt to changes in the environment, which are reflected in the quantity of methyl and cyclopentane moieties (Weijers et al., 2007). Based on a survey of global soils, the degree of methylation (MBT) has been shown to depend primarily on MAAT and soil pH, while the cyclization ratio (CBT) is predominantly related to soil pH (Weijers et al., 2007). Therefore, MBT/CBT and its modified version (e.g., MBT′/CBT) have been established to reconstruct paleotemperatures (Weijers et al., 2007; Peterse et al., 2012). More recently, improved chromatographic techniques have enabled the separation of 5- and 6-methyl brGDGTs, resulting in a set of new brGDGTs proxies, which were used to recalibrate traditionally defined MBT–CBT indices (De Jonge et al., 2014; Yang et al., 2015). Investigations of brGDGTs distributions in lake sediments from sites on the TP have shown that brGDGTs proxies are a reliable means of reconstructing past temperature variability across the TP (Wang et al., 2016; Liang et al., 2022). Specifically, brGDGTs have been successfully applied to TP lake sediments to reconstruct palaeotemperature variations during the Holocene (Li et al., 2017; Feng et al., 2019; Li and Fan, 2019; Wang et al., 2021; Sun et al., 2022; Zhang et al., 2022).

In this study, we obtained a brGDGTs-based paleotemperature record spanning the past 4700 years from Xiada Co on the western TP. We have already reconstructed a 2000-year-long temperature record for Xiada Co using the brGDGTs-based temperature proxy (Index1) (Li et al., 2019). However, as a regional calibration of brGDGTs for TP lakes using the improved separation technique was not available at that time, the ~2000-year-long temperature record from Xiada Co presented in Li et al. (2019) was calculated used a global calibration. However, considering the unique climate and environment of the TP, a regional rather than a global calibration for brGDGTs-based palaeothermometry is clearly needed (Wang et al., 2021). Recently, Liang et al. (2022) analyzed 29 surface sediment samples from lakes in TP using the improved separation technique. They found that all temperature variables had a stronger linear relationship with the degrees of methylation of 6-methyl brGDGTs (MBT'_{6Me}) than 5-methyl brGDGTs ($MBT'_{5Me)}$, which was also found in a survey of the distribution of brGDGTs in 35 lakes across China (Dang et al., 2018). Subsequently, they produced a new MBT'_{6Me}-MAAT calibration based on the 29 surface sediment samples from lakes on the TP, together with 39 additional lake surface sediments from China (Dang et al., 2018). In the present study, we applied the new calibration to a sediment core spanning the last ~5000 years from Xiada Co. Our objectives were to document MAAT variations in the western TP over the past ~5000 years, and to determine the factors that contribute to the spatiotemporal differences of paleotemperature variations across the TP.

2 Study site

Xiada Co (33°23′N, 79°21′E, 4358 m a.s.l) is a small freshwater lake located on the western TP, ~50 km west of the town of Rutog (Fig. 1; Li et al., 2019). The lake is fed mainly by precipitation and glacier meltwater. The results of a modern lake survey indicated that the salinity of the surface lake water is 0.15 g/L, and the pH of the lake water is 8.6. The lake has a surface area of 8 km^2 with a maximum depth of 20 m (Li et al., 2019). A long-term instrumental data series from Shiquanhe meteorological station, ~120 km south-east of Xiada Co, shows that the MAAT was 1.02°C over the 30-year interval of 1981–2010 CE (Wang et al., 2021). The current precipitation in this region is monsoonal, and the

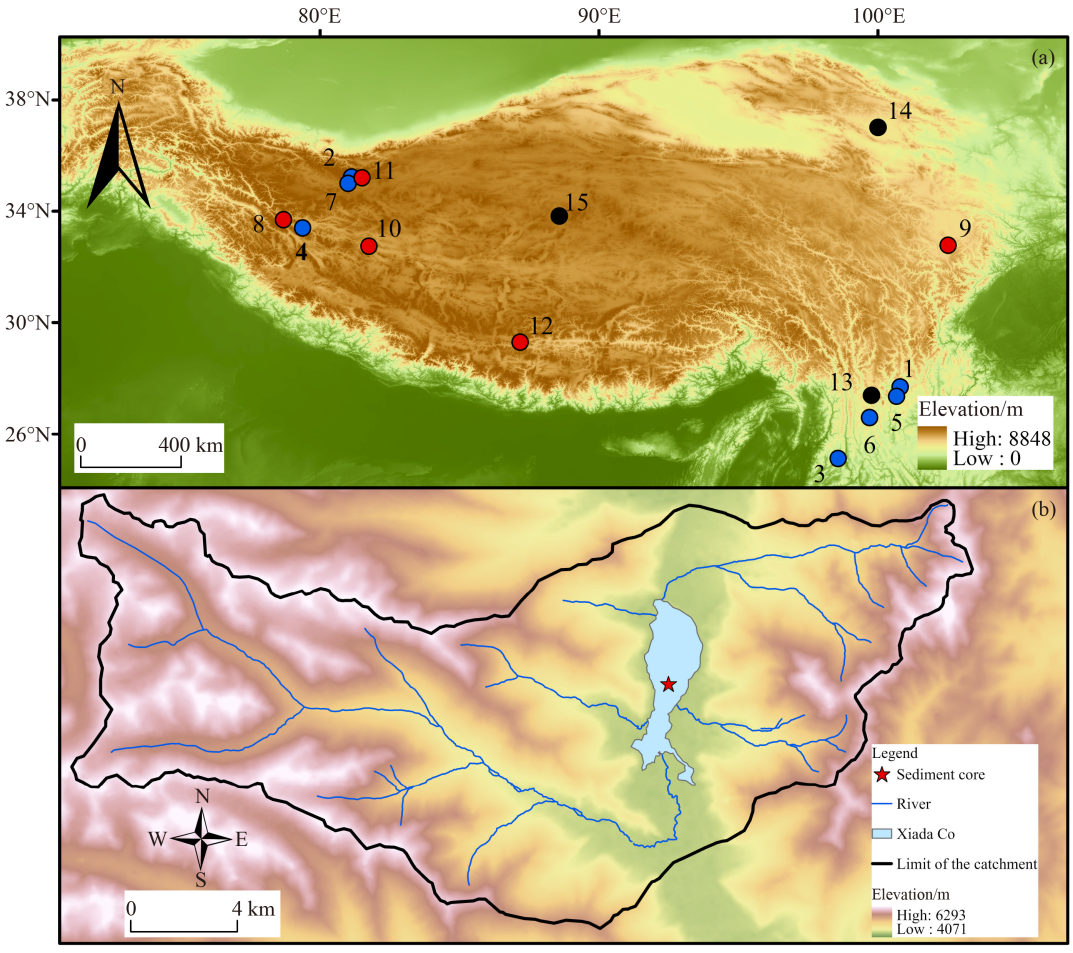

Fig. 1 (a) Map showing the sites referenced in the text: Lugu Lake (1), Chongce ice core (2), Tengchongqinghai Lake (3), Xiada Co (4), Hehai Lake (5), Tiancai Lake (6), Guozha Co (7), Bangong Co (8), Hongyuan Peat (9), Aweng Co (10), Guliya ice core (11), Ngamring Co (12), Cuoqia Lake (13), Qinghai Lake (14), Lingge Co (15), Red circles indicate temperature records showing a long-term warming trend, blue circles indicate temperature records showing a long-term cooling trend, and black circles indicate temperature records with no clear trend. (b) Drainage basin of Xiada Co. The sampling site is represented by a red star at the depocenter at 19 m water depth.

summer rainfall accounts for > 80% of the total annual precipitation (Li et al., 2019).

3 Materials and methods

3.1 Sampling

A 273-cm-long sediment core (XDC2014-1), was collected from the center of Xiada Co at a water depth of 19 m using a Uwitec piston corer (Fig. 1). The upper part of the sediment core was continuously subsampled at an interval of 0.5 cm, and below 100 cm the core was subsampled at an interval of 1 cm. All samples were stored in a freezer prior to laboratory analysis (Li et al., 2019).

3.2 Lipid extraction and brGDGTs analysis

brGDGTs were extracted from the lake sediments using the methods described by Li et al. (2019). Freeze-dried samples (~5 g) were ultrasonically extracted with dichloromethane/methanol (9:1, v/v) (15 min, 3 ×, 30°C). The total extract was chromatographed using an activated Al_2O_3 column (for 2 h at 150°C). The nonpolar and polar fractions (the latter containing GDGTs) were eluted using *n*-hexane/dichloromethane (9:1, v/v) and dichloromethane/methanol (1:1, v/v), respectively. The extracts were concentrated in as stream of nitrogen gas and then dissolved in *n*-hexane/isopropanol (99:1, v/v). A 0.2 μm PTFE filter was used to remove large molecular compounds and particulate matter prior to HPLC-MS analysis.

GDGTs analysis was performed using HPLC-APCI-MS (Agilent 1260 HPLC system with 6100 MS), with autoinjection, at the Institute of Tibetan Plateau Research, Chinese Academy of Sciences (ITPCAS). Separation of 5- and 6-methyl brGDGTs isomers was achieved with three Hypersil Gold Silica LC columns in sequence (each with dimensions of 100 mm × 2.1 mm, 1.9 μm; Thermo

Fisher Scientific, USA). The instrumental setups for HPLC were as follows: column temperature 40°C, injection volume 10 μL, flow rate 0.2 mL/min. GDGTs were eluted isocratically with 84% A and 16% B for the first 5 min, where A is *n*-hexane and B is EtOA, followed by a linear gradient change to 82% A and 18% B from 5 to 65 min and then to 100% B for 21 min, followed by 100% B for 4 min to wash the column, and then back to 84% A and 16% B to equilibrate the column. APCI-MS conditions were as follows: nebulizer pressure 60 psi, vaporizer temperature 400°C, drying gas flow rate 6 L/min and temperature 200°C, capillary voltage 3500 V, corona 5 μA. Detection was performed in selected ion monitoring (SIM) mode via $[M + H]^+$ at m/z 744 for the C_{46} standard, 1302, 1300, 1298, 1296, and 1292 for iGDGTs and 1050, 1048, 1046, 1036, 1034, 1032, 1022, 1020, 1018 for brGDGTs. GDGTs were quantified using an external standard, and the peak areas were manually integrated, assuming an identical response factor for the GDGTs. The definition of the structure and nomenclature of brGDGTs follows Yang et al. (2015).

4 Results and discussion

4.1 Chronology

The chronology of core XDC2014-1 was constructed using ^{210}Pb and ^{137}Cs analyses of the upper 10 cm (Fig. 2(a)), together with 6 AMS ^{14}C ages of total organic carbon from the lower part of the core (Fig. 2(b)). The age-depth model of core XDC2014-1 is discussed in detail in Li et al. (2019). Briefly, ^{210}Pb and ^{137}Cs analyses were conducted by gamma spectrometry, using a high-purity well-type germanium detector (ORTEC GWL-120–15), at the Institute of Tibetan Plateau Research, Chinese Academy of Sciences. The age-depth relationship of the upper 10 cm of the core, together with the dating uncertainty, was established using the constant rate of supply (CRS) model (Appleby and Oldfield, 1978). A ^{137}Cs peak occurs at the depth of 4.5 cm, likely corresponding to the Chernobyl nuclear accident in 1986 CE, which is consistent with the ^{210}Pb dating results. The final chronology for the most recent sediments is based on ^{210}Pb dating (Fig. 2(a)), according to which the upper 10 cm of the core represent the interval of 1919–2013 CE, corresponding to a sedimentation rate of ~0.1 cm/yr.

Because of the lack of terrestrial macrofossils in core XDC2014-1 the AMS ages were obtained from bulk organic carbon. The ^{14}C reservoir ages of lakes on the TP show significant temporal variability, and they can vary by as much as ~5000 years within a single lake between the last deglaciation and the late Holocene, resulting in large age uncertainties in reservoir age corrections (Hou et al., 2012). In addition, large errors may be introduced by assuming a constant sediment accumulation rate if the profile spans significant environmental changes, which can have a major impact on calculating a reservoir effect (Zhou et al., 2014). To reduce the chronological uncertainty, it is advisable to consider the possible temporal changes of ^{14}C reservoir ages and to determine the reservoir age for different sections of the sediment core (Zhou et al., 2014). The differences in the total organic content (TOC) of core XDC2014-2 indicate an abrupt change in the sedimentation rate at the depth of 80 cm. Therefore, to calculate the reservoir ages we divided the core into two sections, with the boundary at 80 cm. All the ^{14}C data were first calibrated to calendar ages using CALIB 7.0.2. Linear regression of the uppermost two calibrated ^{14}C ages yielded an age of 2972 cal yr BP for the depth of 0 cm, which can be regarded as the average reservoir age for the upper section of the core. According

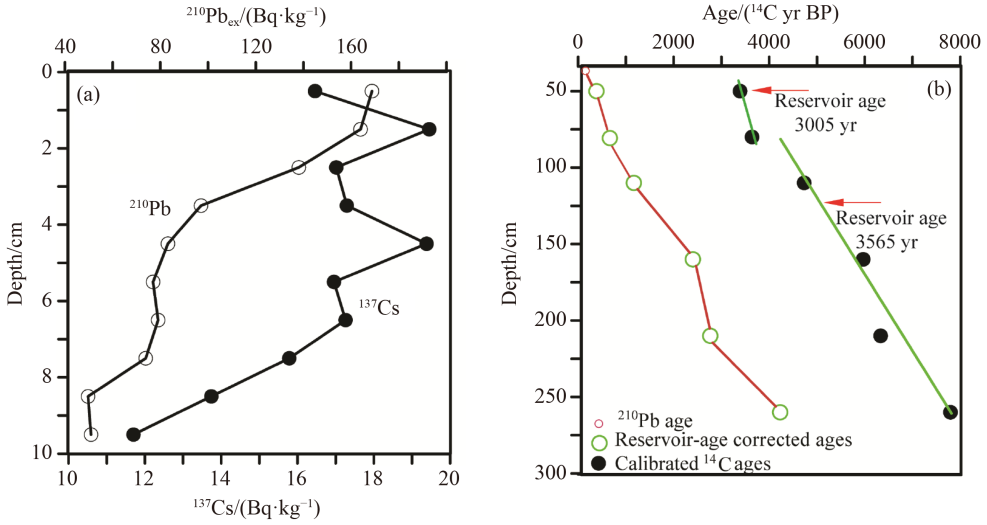

Fig. 2 Age-depth model for core XDC2014-1 adopted from Li et al. (2019). The ages of the upper 10 cm were determined by ^{210}Pb and ^{137}Cs dating (Fig. 2(a)), and those of the lower part by AMS ^{14}C dating (Fig. 2(b)).

to the ^{210}Pb dating results, the depth of 8 cm has the age of 0 yr BP (1950 CE), while 3038 cal yr BP is inferred from the extrapolation of the upper two radiocarbon dates. Thus, 3038 years can also be regarded as the reservoir age at that depth. We used the mean value for the two reservoir ages (3005 years) as the reservoir age for the upper section of the core. Subsequently, a linear fit was applied to the lower four calibrated ^{14}C ages which yielded a ^{14}C age of 4199 cal yr BP for the depth of 80 cm, while the reservoir age–corrected ^{14}C age at the depth of 80 cm was 634 cal yr BP. Therefore, we took the difference (3565 years) between the two ages as the reservoir age below 80 cm. All the reservoir ages were then subtracted from the original calibrated ages and the final chronology for the sediment core was constructed based on the 6 reservoir age–corrected ^{14}C ages together with the ^{210}Pb/^{137}Cs chronology for the upper 10 cm. Linear interpolation between the reservoir age-corrected ages was used to obtain the ages of all the sediment subsamples (Wu et al., 2013).

4.2 Distribution and source of brGDGTs in the sediments of Xiada Co

The 5- and 6-methyl brGDGTs in all samples were chromatographically separated. Non-cyclopentane moieties (IIIa, IIIa′, IIa, IIa′, and Ia) dominate the distribution of brGDGTs, contributing 83% of the total amount within the core samples (Fig. 3(a)). The relative abundances of brGDGTs containing 1–2 cyclopentane moieties were relatively low and sometimes too low to detect. The most abundant brGDGTs are pentamethylated brGDGTs (41%), followed by hexamethylated (38%) and tetramethylated (21%) brGDGTs.

To further evaluate the applicability of brGDGTs-based proxies in Xiada Co, it is necessary to determine the source of the brGDGTs within the lake (Naeher et al., 2014). Hence, we compared the brGDGTs in the sediments from Xiada Co with published data from Tibetan soils (Ding et al., 2015) and lake sediments (Liang et al., 2022). The results demonstrate that the non-cyclopentane moieties (IIIa, IIIa′, IIa, IIa′, and Ia) dominate the distribution of brGDGTs in all samples (Fig. 3(a)). In addition, all are dominated by pentamethylated brGDGTs, followed by hexamethylated brGDGTs and tetramethylated brGDGTs. Nevertheless, there are subtle differences; for example, the brGDGTs in the sediments samples from Xiada Co and the sediments of other Tibetan Plateau lakes have a lower fractional abundance of pentamethlyated brGDGTs (41% for Xiada Co and 44% for the other Tibetan lake sediments) relative to the Tibetan Plateau soils (54%), but a higher fractional abundance of hexamethylated brGDGTs (38% for Xiada Co down-core and 39% for the other Tibetan lake sediments) relative to the Tibetan soils (27%). This indicates that the brGDGTs in the core sediments from

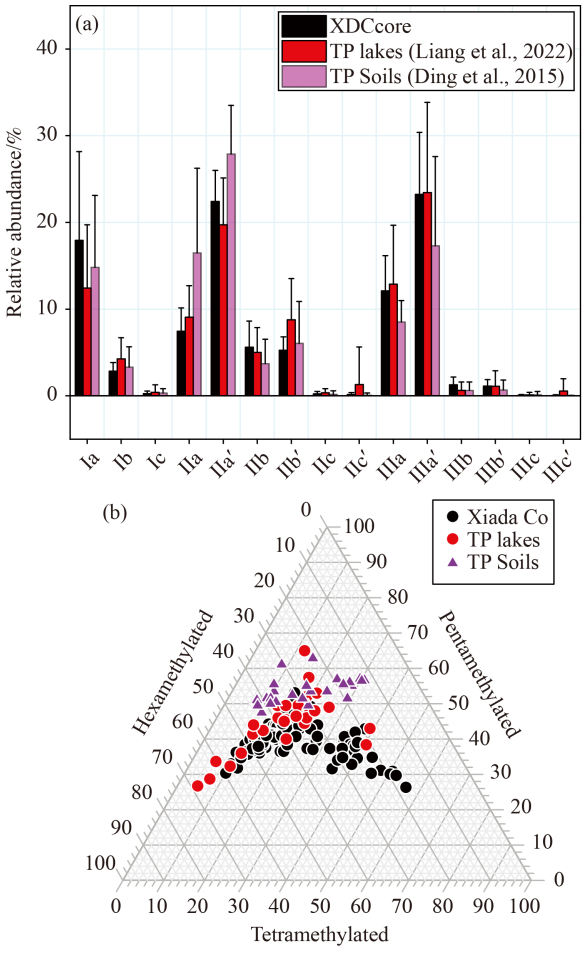

Fig. 3 (a) Comparison of the fractional abundance of brGDGTs in core XDC2014-1 for Xiada Co (black, this study) with that in soils (purple, Ding et al., 2015) and lake surface sediments (red, Liang et al., 2022) from the Tibetan Plateau. (b) Comparison of the fractional abundances of tetramethylated, pentamethylated, and hexamethylated brGDGTs in the sediments from Xiada Co with lake surface sediments (Liang et al., 2022) and soils (Ding et al., 2015) from the Tibetan Plateau, and globally distributed soils (Naafs et al., 2017).

Xiada Co are generally of *in situ* origin and that the terrestrial input if brGDGTs is negligible. Also, the ternary diagram of tetra-, penta-, and hexa-methylated brGDGTs can separate soil-derived brGDGTs from those of in situ (aquatic) origin (Sinninghe Damsté, 2016). In a ternary plot, the data from Xiada Co are distributed close to those of other Tibetan lake sediments, but they are distinguished from Tibetan soils (Ding et al., 2015) and global soils (Naafs et al., 2017) (Fig. 3(b)). This further indicates that that the brGDGTs from Xiada Co are mainly produced within the water column.

4.3 Late Holocene temperature reconstruction for Xiada Co

We reconstructed the temperature variations in Xiada Co using both soil-based (Weijers et al., 2007; Peterse et al., 2012; De Jonge et al., 2014; Ding et al., 2015) and lake-

specific (Günther et al., 2014; Wang et al., 2016; Liang et al., 2022) functions on global and regional scales. The formulas used to calculate the brGDGTs indices and calibrations are shown in Table 1. Generally, the temperature reconstructions show a similar trend of variation but with different absolute values (Fig. 4). Among these calibrations, that of Liang et al. (2022) appears to be the most reliable because the current temperature calculated by this function (1.5°C) is close to the MAAT from 2011 to 2014 at Shiquanhe Meteorological station (1.6°C). Additionally, comparison of the MBT'_{6Me}-reconstructed MAAT with the nearby meteorological data set spanning the past 37 years indicates a significant correlation between the two, both showing a minimum at ~2000 CE and relatively high MAAT before and after 2000 CE (Liang et al., 2022). In addition, this calibration provides the most extensive coverage of Tibetan lakes (31 lakes), increasing our confidence in applying it to lakes on the TP. Therefore, we adopted the MBT'_{6Me} -MAAT relationship developed by Liang et al. (2022) to convert the data from Xiada Co to MAAT.

As shown in Fig. 4(a), the brGDGTs-based MAAT record from Xiada Co has an average of ~2.8°C, with the range of around –2.1°C–13.0°C over the past 4700 years. Specifically, the MAAT shows a general cooling trend during the past 4700 years. A relatively warm interval is evident during ~4700–2200 cal yr BP, with MAAT fluctuating between 5.3°C and 13.0°C. The MAAT then decreased by ~4.4°C at ~2100 cal yr BP, and it continued to decrease to the present-day with centennial-scale oscillations superimposed, centered at ~800 cal yr BP, ~600 cal yr BP, and ~190–170 cal yr BP. MAAT decreased abruptly at ~500–300 cal yr BP, reaching the lowest average annual temperature in the lake over the past 4700 years.

Several researchers have proposed a temporal consistency between climatic events and the evolution of human civilization, implying a causal relationship (deMenocal, 2001; Zhang et al., 2010; Kennett et al., 2012). Furthermore, several studies have suggested that climate change played a role in the transitions between dynasties and the associated societal evolution in China (Yancheva et al., 2007). Thus, high-resolution climate records are potentially valuable for improving our understanding of the impacts of past climate change on human societies. Xiada Co is located near the ruins of the Guge Kingdom, which was established in the mid-10th century in the western TP and flourished for ~700 years (Kathayat et al., 2017). However, the Guge Kingdom abruptly collapsed in the 17th century, which was ascribed to an aridification trend caused by a monsoonal minimum (Cheng et al., 2010; Kathayat et al., 2017; Li et al., 2019). The brGDGTs-based temperature record from Xiada Co suggests that the temperature decreased abruptly at ~500–300 cal yr. The decreased crop yield potentially caused by this temperature decrease may have contributed to the collapse of the Guge Kingdom (Liang et al., 2022). Additionally, this temperature decrease was synchronous with a major decline in the human population reflected by changes in the absolute concentrations of fecal stanols in core XDC2014-1 from Xiada Co (Li et al., 2023c), which also indicates that abrupt climate change may have contributed to the collapse of the Guge Kingdom. However, possible errors and uncertainties associated with the ^{14}C chronology for core XDC2014-1 necessitate caution in establishing a correlation between temperature changes and the evolution of regional civilizations, and further research is needed to constrain the sedimentary chronology for Xiada Co.

Table 1 Formulas used to calculate the brGDGTs indices and calibrations

Index	Definition	Reference
MBT	MBT=(Ia+Ib+Ic)/(Ia+Ib+Ic+IIa+IIa'+IIb+IIb'+IIc+IIc' +IIIa+IIIa'+IIIb+IIIb'+IIIc+IIIc')	Naafs et al. (2017)
MBT'	MBT'=(Ia+Ib+Ic)/(Ia+Ib+Ic+IIa+IIb+IIc+IIIa+IIa'+IIb'+IIc'+IIIa')	De Jonge et al. (2014)
CBT	CBT= –log[(Ib+ IIb+ IIb')/(Ia+ IIa+ IIa')]	De Jonge et al. (2014)
MBT'_{5ME}	MBT'_{5ME} =(Ia+Ib+Ic)/(Ia+Ib+Ic+IIa+IIb+IIc+IIIa)	De Jonge et al. (2014)
$MBT_{5/6}$	$MBT_{5/6}$ = (Ia+Ib+Ic+IIa')/(Ia+Ib+Ic+IIa+IIb+IIc+IIIa+IIIa')	Ding et al. (2015)
MBT'_{6ME}	MBT'_{6ME} =(Ia+Ib+Ic)/(Ia+Ib+Ic+IIa'+IIb'+IIc'+IIIa')	Dang et al. (2018)
Material	**Function**	**Reference**
Tibetan Planteau lakes	MAAT= –3.75+40.92×MBT–6.03×CBT	Wang et al. (2016)
Global soils	MAAT= –6.1+50×MBT–9.35×CBT	Weijers et al. (2007)
Global soils	MAAT = 0.81–5.67×CBT + 31.0×MBT'	Peterse et al. (2012)
Tibetan soils	$MAT= –20.14+39.51\times MBT_{5/6}$	Ding et al. (2015)
Global soils	$MAT= –8.57+31.45\times MBT'_{5ME}$	De Jonge et al. (2014)
Tibetan lakes	MAAT= –3.84+5.92×MBT'+9.84×CBT	Günther et al. (2014)
Tibetan Planteau lakes	$MAAT= 30.47\times MBT'_{6ME} – 5.92$	Liang et al. (2022)

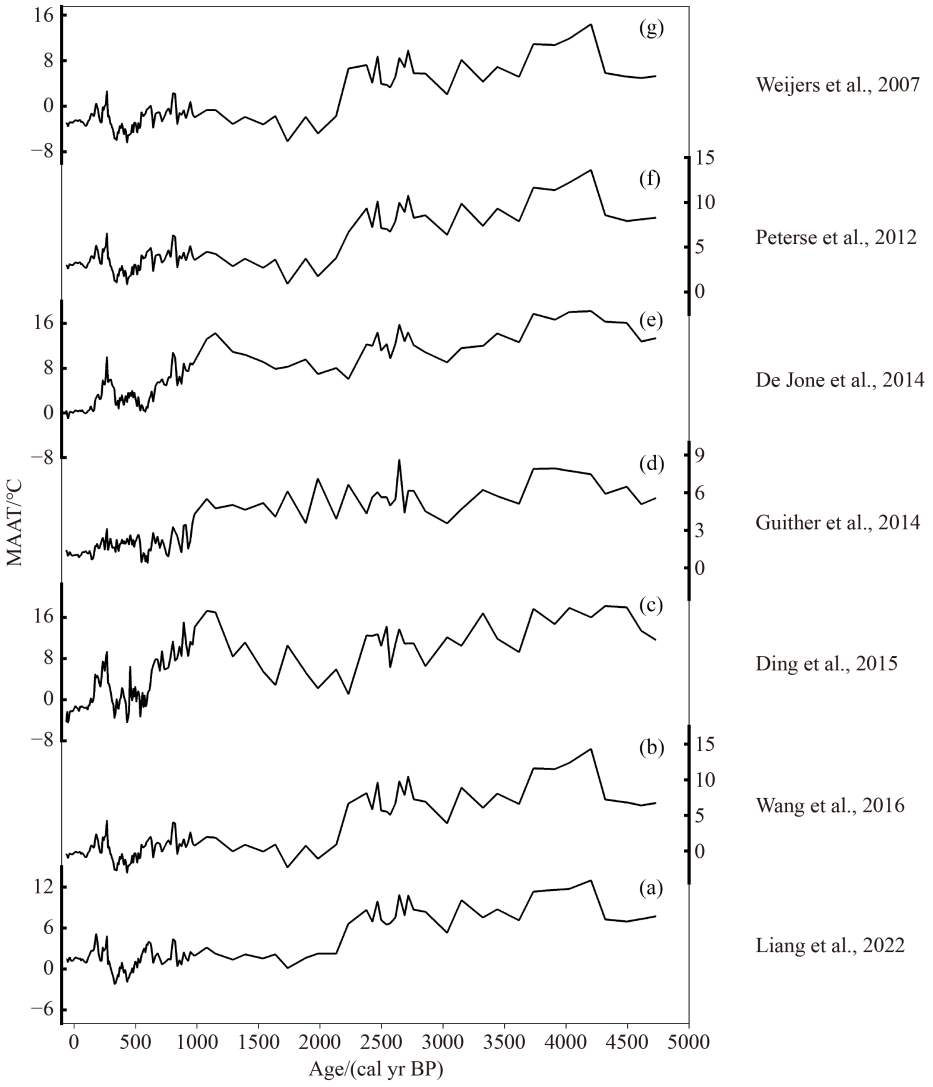

Fig. 4 Comparison of MAAT records for Xiada Co reconstructed using different calibrations: (a) MAAT based on Tibetan Lakes proposed by Liang et al. (2022), which is adopted in this study; (b) MAAT based on Tibetan Lakes proposed by Wang et al. (2016); (c) MAAT based on Tibetan soil proposed by Ding et al.(2015); (d) MAAT based on Tibetan Lakes proposed by Günther et al. (2014); (e) MAAT based on global soils proposed by De Jonge et al. (2014); (f) MAAT based on global soils proposed by Peterse et al. (2012); (g) MAAT based on global soils proposed by Weijers et al. (2007).

4.4 Pattern of temperature changes on the TP over the past 5000 years

Our reconstructed MAAT record from Xiada Co indicates a cooling trend with an abrupt temperature decrease at ~500–300 cal yr BP (Fig. 5(a)). To further evaluate our record, we compared it with other paleoclimate records from the TP and adjacent areas. The criteria we used for selecting these records was that they were quantitative and were interpreted by the authors as having a clear seasonal significance.

Changes in the MAAT on the TP during the past 5000 years have been reconstructed using various temperature proxies, including pollen assemblages (e.g., Chen et al., 2020), ice core $\delta^{18}O$ (e.g., Thompson et al., 1997; Pang et al., 2020), and brGDGTs (e.g., Li et al., 2017; He et al., 2020; Wang et al., 2021; Zhao et al., 2021). Unfortunately, some of these reconstructions are mutually inconsistent (Fig. 5). A cooling trend over the past ~5000 years has been reported by several recent studies; for example, Chen et al. (2020) compiled a set of pollen data for the TP (Fig. 5(e)) and found that the annual temperature gradually decreased since the middle Holocene. In addition, the temperature anomalies reconstructed from the $\delta^{18}O$ record of the Chongce ice core, which has a slight winter bias, show a cooling trend during the past 5000 years (Fig. 5(f)) (Pang et al., 2020). Likewise, brGDGTs records from Tengchongqinghai lake (Fig. 5(b)) and Lugu lake (Fig. 5(c)) (Zhao et al., 2021), in the Hengduan Mountains on the south-eastern margin of the TP, also depict cooling trend from the middle Holocene. The similarity of the temperature records from

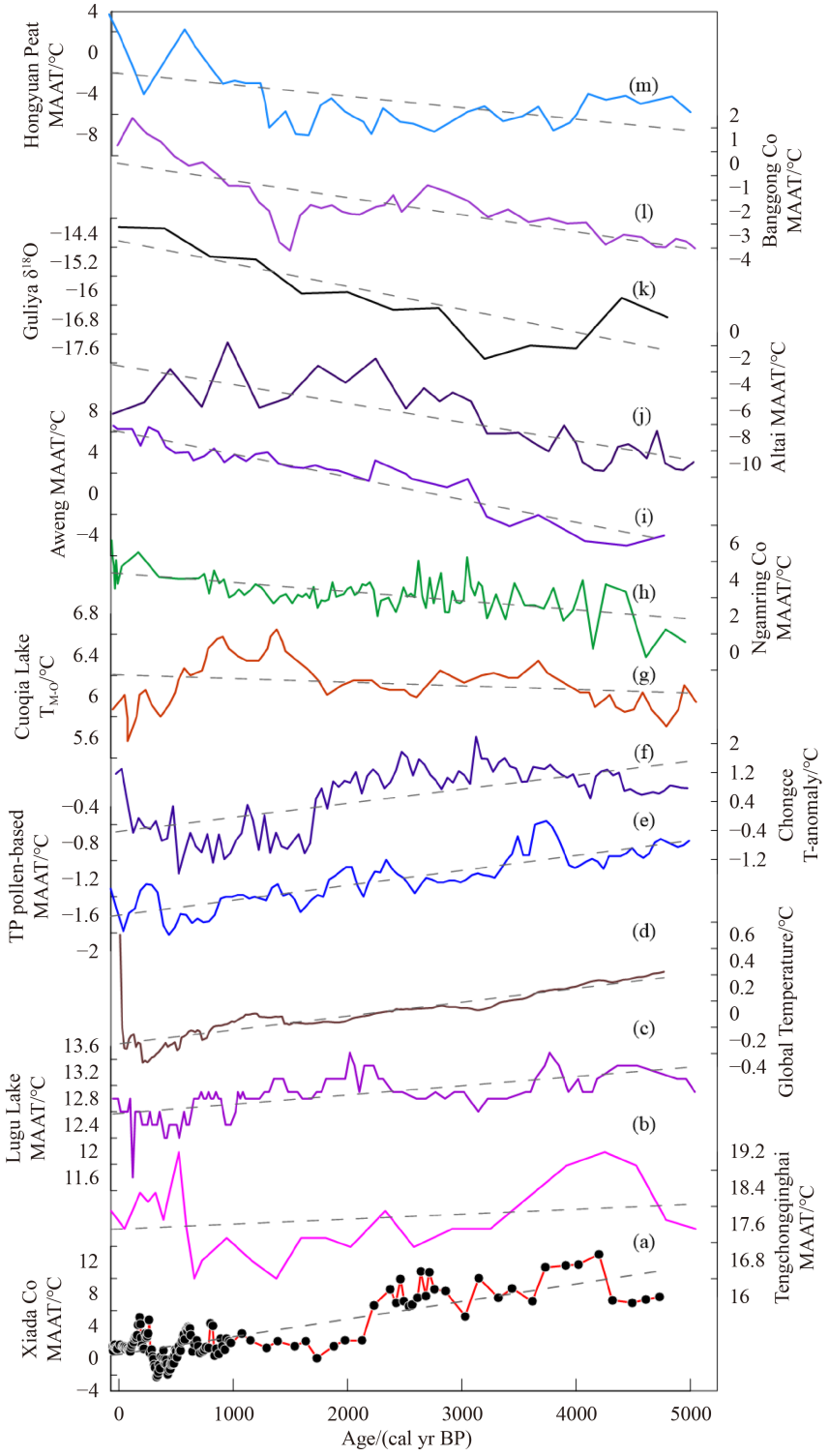

Fig. 5 Comparison of brGDGTs-based MAAT at Xiada Co (a) with brGDGTs-based MAAT reconstruction for Tengchongqinghai Lake (Zhao et al., 2021) (b); brGDGTs-based MAAT reconstruction for Lugu Lake (Zhao et al., 2021) (c); global temperature reconstructions (Marcott et al., 2013) (d); MAAT reconstructed by a synthesis of fossil pollen records from the TP (Chen et al., 2020) (e); brGDGTs-based temperature reconstruction for Chongce ice core (Pang et al., 2020) (f); brGDGTs-based ice-free-season temperature (from March to October, $T_{M\text{-}O}$) reconstruction for Cuoqia Lake (Zhang et al., 2022) (g); brGDGTs-based MAAT reconstruction for Ngamring Co (Sun et al., 2022) (h); brGDGTs-based MAAT reconstruction for Aweng Co (Li et al., 2017) (i); brGDGTs-based MAAT reconstruction from the alpine Sahara sand peatland in the southern Altai Mountains (Wu et al., 2020) (j); $\delta^{18}O$ record of the Guliya ice cap (Thompson et al., 1997) (k); brGDGTs-based MAAT reconstruction for Bangong Co (Wang et al., 2021) (l); brGDGTs-based MAAT reconstruction for the Hongyuan peatland (Yan et al., 2021) (m).

Xiada Co (Fig. 5(a)), Tengchongqinghai lake (Fig. 5(b)) and Lugu lake (Fig. 5(c)) suggest that MAAT variations were synchronous in the western and south-eastern TP, and compatible with the global trend indicated by proxy-based paleotemperature syntheses (Fig. 5(d)) (Marcott et al., 2013). However, the ice core $\delta^{18}O$ record from the Gulliya ice core shows a long-term warming trend during the middle to late Holocene (Fig. 5(k)) (Thompson et al., 1997), which differs from our MAAT record and from other TP temperature records, including those from the Chongce ice cap (Fig. 5(f)), Tengchongqinghai lake (Fig. 5(b)) and Lugu lake (Fig. 5(c)). Furthermore, the brGDGTs-based MAAT records from Bangong Co (Fig. 5(l)) (Wang et al., 2021) and Aweng Co (Fig. 5(i)) (Li et al., 2017) on the western margin of the TP; from Ngamring Co on the southern TP (Fig. 5(h)) (Sun et al., 2022); and from the Hongyuan peatland on the eastern TP (Fig. 5(m)) (Yan et al., 2021) all demonstrate a warming trend during the past 5000 years. In addition, beyond the TP, a peat record from the Altai Mountains (Fig. 5(j)) also shows distinct temperature increase during the past 5000 years (Wu et al., 2020). The warming trend since ~5000 years cal yr BP reflected by these temperature records is completely at variance with our brGDGTs-based temperature reconstruction from Xiada Co. It should be noted that brGDGTs-based MAAT records do not consistently show a prominent warming or cooling trend during the past ~5000 years. For example, although the MAAT record from Lingge Co on the central TP fluctuated sharply during the past 5000 years, there was only a weak overall warming trend (He et al., 2020). Furthermore, the ice-free-season temperature (from March to October, $T_{M\text{-}O}$) based on brGDGTs from Cuoqia Lake (Fig. 5(g)), in the hinterland of the Hengduan Mountains on the south-eastern margin of TP, shows a relatively stable pattern during 5000–1500 cal yr BP (Fig. 5(g)) (Zhang et al., 2022), which differs from the record from Xiada Co and from other brGDGTs-based temperature records.

Summer temperature changes have been reconstructed from chironomids (Chang et al., 2017; Zhang et al., 2017), pollen (Chen et al., 2020), and alkenones (Wang et al., 2015b; Hou et al., 2016). Our brGDGTs-based temperature record from Xiada Co (Fig. 6(a)) demonstrates a similar trend to the pollen–based summer temperature record (Fig. 6(b)) (Chen et al., 2020), displaying a gradual cooling trend during the past 5000 years. Likewise, the summer temperature variability inferred from subfossil chironomid assemblages from Heihai Lake (Fig. 6(c)) and Tiancai Lake (Fig. 6(g)), on the south-eastern margin of the TP, shows a generally decreasing trend for the past 5000 years, suggesting that summer temperatures on the south-eastern margin of the TP primarily responded to changes in the Asian summer monsoon, on the millennial scale (Chang et al., 2017). Similarly, Chen et al. (2020) summarized the activity of Holocene glaciers based on the published ^{10}Be ages of moraines on the TP and in the surrounding mountains. The increased activity of Tibetan glaciers since ~5000 cal yr BP suggests that glacier accumulation occurred in response to decreasing summer temperatures (Fig. 6(e)). Moreover, the $\delta^{18}O$ values of authigenic carbonate at Guozha Co gradually became enriched from the middle Holocene onward, reaching a maximum during 1500–500 cal yr BP (Fig. 6(d)), which indicates a decrease in glacier meltwater influx to the lake since the middle Holocene, which can be attributed to decreasing summer temperatures (Li et al., 2021b). It should be mentioned that the alkenone-based summer temperature record from Lake Qinghai shows an interval of sustained summer temperature decrease during 5000–3500 cal yr BP, after which summer temperatures gradually increased to the current level, with several fluctuations superimposed (Fig. 6(f)) (Hou et al., 2016), which differs from our record from Xiada Co and from other summer temperature records.

In summary, although the absolute values are different, the trends of the temperature record from Xiada Co is consistent with most summer temperature records (Chang et al., 2017; Zhang et al., 2017; Chen et al., 2020; Li et al., 2021b) and with some of the MAAT records (Chen et al., 2020; Pang et al., 2020; Zhao et al., 2021) from the TP—all demonstrating a cooling trend during the past 5000 years. However, several other MAAT records from the TP contrast with our temperature records, showing a marked warming trend since the middle Holocene (Thompson et al., 2006; Li et al., 2017; Wang et al., 2021; Yan et al., 2021; Sun et al., 2022). This discrepancy may partly reflect the spatiotemporal complexity of temperature variations on the TP (He et al., 2020). Furthermore, the climate series collected from different regions of the TP are derived from multiple proxy types, each with specific principles, procedures, and potentially unique qualities. Thus, the biases inherent in each proxy archive, such as seasonality and chronological error, may be a major source of inconsistency in the reconstructed temperature series.

4.5 Possible causes of the spatial heterogeneity of temperature changes on the TP

Evaluating these paleotemperature reconstructions for the TP for the past 5000 years is potentially complicated. The discrepancies between these temperature records could be related to seasonality effects on the temperature proxies (Liu et al., 2014; Hou et al., 2019a; Wang et al., 2021; Feng et al., 2022). Many temperature proxies (such as brGDGTs, pollen, and alkenones) are controlled by seasonal processes and reflect the climate of the growing season (Chu et al., 2012). Therefore, seasonal biases exist for these indicators and thus for the resulting temperature reconstructions. This seasonal bias may be especially

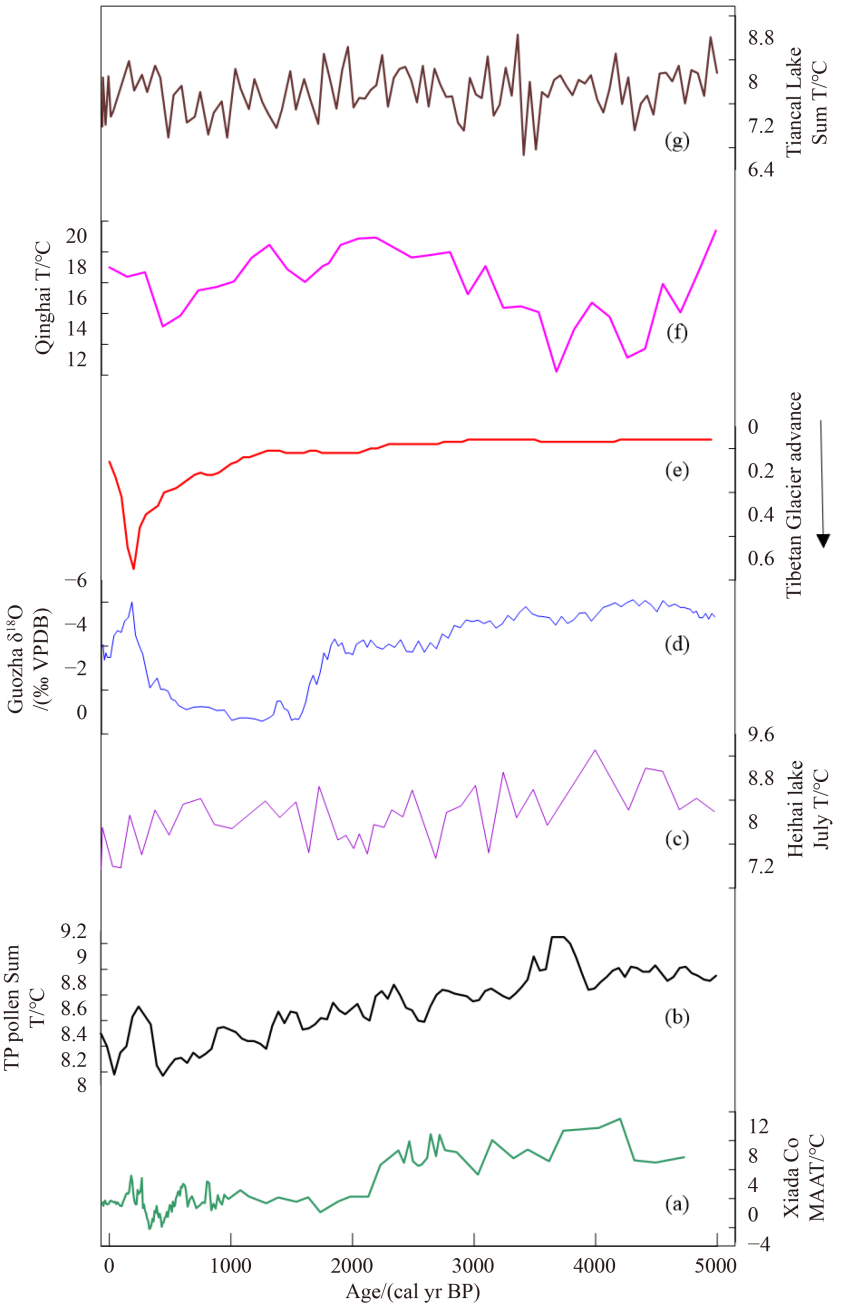

Fig. 6 Comparison of brGDGTs-based MAAT at Xiada Co (a) with summer temperature reconstructed by a synthesis of fossil pollen records from the TP (Chen et al., 2020) (b); summer temperature inferred from subfossil chironomid assemblages from Heihai Lake (Chang et al., 2017) (c); $\delta^{18}O$ record of Guozha Co (Li et al., 2021b) (d); probability density plot of moraine ages on the TP (Chen et al., 2020) (e); alkenone-based summer temperature for Qinghai Lake (Hou et al., 2016) (f); summer temperature inferred from subfossil chironomid assemblages from Tiancai Lake (Zhang et al., 2017) (g).

pronounced in the arid, high-elevation TP region, where the modern climate is characterized by strong temperature seasonality with a long cold season and a short mild season (Li et al., 2011). For example, the chironomid-based summer temperature records from Tiancai Lake (Zhang et al., 2017) and Heihai Lake (Chang et al., 2017) show a gradual cooling trend during the past 5000 years Similar characteristics are shown by a pollen-based summer temperature synthesis for the TP (Chen et al., 2020). By contrast, the brGDGTs-based MAAT records from Bangong Co (Wang et al., 2021), Aweng Co (Li et al., 2017), Ngamring Co (Sun et al., 2022), and the Hongyuan peatland on the TP (Yan et al., 2021) all show a warming trend during the past 5000 years.

Modern investigations have confirmed the validity of brGDGTs as an MAAT proxy for both soil and lakes in the TP (Günther et al., 2014; Ding et al., 2015; Wang et al., 2016; Liang et al., 2022), and brGDGTs-based

proxies have been increasingly used for MAAT reconstruction from lake sediments on the TP (Li et al., 2017, 2019; Feng et al., 2019; He et al., 2020; Wang et al., 2021; Zhao et al., 2021; Sun et al., 2022). However, brGDGTs proxy estimates are sometimes assumed to have a seasonal bias (Sun et al., 2011; Deng et al., 2016; Foster et al., 2016; Dang et al., 2018; Qian et al., 2019; Zhu et al., 2021). An investigation of alkaline lake sediments from cold regions in China has verified a warm-season bias in brGDGTs production (Dang et al., 2018), which is consistent with numerous other studies indicating a bias toward the warm months in mid- to high-latitude lakes (Sun et al., 2011; Shanahan et al., 2013; Foster et al., 2016). Recent studies suggest that whether the lakes freeze and the duration of ice cover can affect the seasonality of the reconstructed temperature (Zhu et al., 2021; Zhang et al., 2022). An analysis of brGDGTs from Sihailongwan maar lake (Lake SHL) in NE China showed that the brGDGTs are produced predominantly in summer and autumn due to the long duration of ice cover, from the middle of November to the end of April (Zhu et al., 2021). Likewise, a recent study suggested that the brGDGTs in Cuoqia Lake on the TP reflect the temperature of the ice-free-season (from March to October, $T_{M\text{-}O}$), with freezing occurring during the cold season (Zhang et al., 2022). For Xiada Co, located in a higher altitude area of the western TP, mean temperatures above freezing occur consecutively during the five months from May to September, as indicated by observations from the nearby Shiquanhe station. Thus, the brGDGTs-reconstructed annual temperature record from at Xiada Co predominantly reflects air temperature changes during the ice-free season from May to September, suggesting that a possible warm season bias exists in our reconstruction. This may partly explain why the trend of the Xiada Co temperature record is consistent with most of the summer temperature records from the TP (Chang et al., 2017; Zhang et al., 2017; Chen et al., 2020; Li et al., 2021b).

However, Drotz et al. (2010) proposed that microbes are able to maintain both catabolic and anabolic processes under freezing conditions, with continuing brGDGTs production occurring even in cold conditions. Moreover, a study of two soil sites in China with contrasting temperature seasonality failed to detect a significant bias toward summer temperature in brGDGTs (Lei et al., 2016). Additionally, no seasonal trends were observed in the concentration and distribution of the branched GDGTs in mid-latitude soils, implying the absence of a seasonal bias in brGDGTs-reconstructed temperatures (Weijers et al., 2011). Measurements of soils and the lake water column also failed to reveal any seasonal trend in the distribution of brGDGTs (Cao et al., 2018). However, recent studies have indicated that brGDGTs-reconstructed MAAT on the TP may be strongly influenced by winter temperatures (Li et al., 2017; Wang et al., 2021; Sun et al., 2022). Therefore, there is still no consensus on whether there is a significant bias toward warm (or colder) months, which contributes to the difficulty in interpreting temperature reconstructions for the TP. There are also unanswered questions regarding a seasonal bias of alkenone-based temperature variations (Zhang et al., 2022). Thus, there is an urgent need to obtain a deeper understanding of the seasonality effects inherent in each proxy, associated with their biosynthesis differences.

Transfer functions between temperature proxies (such as brGDGTs and alkenones) and their living environment are an effective method for reconstructing past climate change. It is essential that the calibration model is chosen carefully since the choice of calibration affects both the trend and absolute values of the reconstructed temperature (Foster et al., 2016; Wang et al., 2021; Sun et al., 2022). For example, Wang et al. (2021) applied a brGDGTs-derived proxy to MAAT reconstruction at Banggong Co using different regional calibrations (Tierney et al., 2010; Sun et al., 2011; Günther et al., 2014; Wang et al., 2016) and concluded that the record based on the function of Günther et al. (2014) demonstrated a different pattern of temperature change compared with the other functions. A similar result was found for Ngamring Co (Sun et al., 2022). Likewise, Zhang et al. (2022) used all the brGDGTs-temperature calibrations published in previous studies based on the improved separation technique (Dang et al., 2018; Russell et al., 2018; Feng et al., 2019; Zhao et al., 2021) to reconstruct temperature changes for core CQ1 during the past 60 years; they found that three regional calibrations resulted in a cooling trend, while another calibration resulted in a warming trend. Therefore, the choice of transfer function may also increase the uncertainty of temperature reconstructions, although it has a more significant effect on the absolute temperature than on the temperature trend. This suggests that a regional rather than a global transfer function is needed, considering the unique climate and environment of the TP.

Chronological errors can also affect the interpretation of past climate and environmental changes on the TP (Hou et al., 2012; Hou et al., 2019b; Wang et al., 2022). Thus, the discrepancies among the available paleotemperature records for the TP during the past 5000 years could result from seasonality effects on the temperature proxies, the length of the freezing season of the lakes, the choice of proxy-temperature calibrations, and chronological errors. Further studies with model simulations are needed to address this issue.

5 Conclusions

We have obtained a brGDGTs-based MAAT record from Xiada Co, with the objective of improving our understanding of the temperature history of the western

TP over the past ~5000. This record indicates a cooling trend with an abrupt temperature decrease during ~500–300 cal yr BP, which may be linked to the collapse of the Guge Kingdom in the 17th century. A comparison of various late Holocene paleotemperature temperature records for the TP, including that from Xiada Co, reveals conflicting results. Moreover, even the brGDGTs-based MAAT series for the TP are inconsistent. We suggest that the seasonality of the temperature proxies, the length of the freezing season of the lakes, the choice of proxy-temperature calibration, and chronological errors may all contribute to the divergent patterns of temperature changes observed for the TP. Hence, there is an urgent need to develop an increased number of high-quality quantitative palaeotemperature series for the TP, which have unambiguous seasonality, site-specific proxy-temperature calibrations, and robust dating.

Acknowledgments This work was financially supported by the National Natural Science Foundation of China (Grant No. 41901105), the Research and Practice Project of Teaching Reform in universities of Henan Province (No. 2022SYJXLX062), the Key Scientific and Technological Research Project of Henan Province (No. 222102320128), the Training Plan of young backbone teachers in Henan Colleges and universities (Nos. 2020GGJS158, 2023GGJS096), and the Nanhu Scholars Program for Young Scholars of XYNU. We thank the editors and three anonymous reviewers for their contractive comments. We appreciate Dr. Jan Bloemendal for English language improvement.

Competing interests The authors declare that they have no competing interests.

References

Appleby P G, Oldfield F (1978). The calculation of lead-210 dates assuming a constant rate of supply of unsupported ^{210}Pb to the sediment. Catena, 5(1): 1–8

Bolch T, Kulkarni A, Kääb A, Huggel C, Paul F, Cogley J G, Frey H, Kargel J S, Fujita K, Scheel M, Bajracharya S, Stoffel M (2012). The state and fate of Himalayan glaciers. Science, 336(6079): 310–314

Braconnot P, Harrison S P, Kageyama M, Bartlein P J, Masson-Delmotte V, Abe-Ouchi A, Otto-Bliesner B, Zhao Y (2012). Evaluation of climate models using palaeoclimatic data. Nat Clim Chang, 2(6): 417–424

Bradley R S, Vuille M, Diaz H F, Vergara W (2006). Threats to water supplies in the tropical Andes. Science, 312(5781): 1755–1756

Cao M, Rueda G, Rivas-Ruiz P, Trapote M C, Henriksen M, Vegas-Vilarrúbia T, Rosell-Melé A (2018). Branched GDGT variability in sediments and soils from catchments with marked temperature seasonality. Org Geochem, 122: 98–114

Chang J, Zhang E, Liu E, Shulmeister J (2017). Summer temperature variability inferred from subfossil chironomid assemblages from the south-east margin of the Qinghai–Tibetan Plateau for the last 5000 years. Holocene, 27(12): 1876–1884

Chen D, Xu B, Yao T, Guo Z, Cui P, Chen F, Zhang R, Zhang X, Zhang Y, Fan J, Hou Z, Zhang T (2015). Assessment of past, present and future environmental changes on the Tibetan Plateau. Chin Sci Bull, 60: 3025–3035

Chen F, Zhang J, Liu J, Cao X, Hou J, Zhu L, Xu X, Liu X, Wang M, Wu D, Huang L, Zeng T, Zhang S, Huang W, Zhang X, Yang K (2020). Climate change, vegetation history, and landscape responses on the Tibetan Plateau during the Holocene: a comprehensive review. Quat Sci Rev, 243: 106444

Cheng H, Edwards R L, Haug G H (2010). Comment on “On linking climate to Chinese dynastic change: spatial and temporal variations of monsoonal rain”. Chin Sci Bull, 55(32): 3734–3737

Chu G, Sun Q, Wang X, Liu M, Lin Y, Xie M, Shang W, Liu J (2012). Seasonal temperature variability during the past 1600 years recorded in historical documents and varved lake sediment profiles from northeastern China. Holocene, 22(7): 785–792

Dang X, Ding W, Yang H, Pancost R D, Naafs B D A, Xue J, Lin X, Lu J, Xie S (2018). Different temperature dependence of the bacterial brGDGT isomers in 35 Chinese lake sediments compared to that in soils. Org Geochem, 119: 72–79

De Jonge C, Hopmans E C, Zell C I, Kim J H, Schouten S, Sinninghe Damsté J S (2014). Occurrence and abundance of 6-methyl branched glycerol dialkyl glycerol tetraethers in soils: implications for palaeoclimate reconstruction. Geochim Cosmochim Acta, 141: 97–112

deMenocal P B (2001). Cultural responses to climate change during the late Holocene. Science, 292(5517): 667–673

Deng L, Jia G, Jin C, Li S (2016). Warm season bias of branched GDGT temperature estimates causes underestimation of altitudinal lapse rate. Org Geochem, 96: 11–17

Ding S, Xu Y, Wang Y, He Y, Hou J, Chen L, He J S (2015). Distributions of branched glycerol dialkyl glycerol tetraethers in surface soils of the Qinghai-Tibetan Plateau: implications of brGDGTs-based proxies in cold and dry regions. Biogeosciences, 12(11): 3141–3151

Drotz S, Sparrman T, Nilsson M, Schleucheret J, Öquist M (2010). Both catabolic and anabolic heterotrophic microbial activity proceed in frozen soils. In: Proceedings of the National Academy of Sciences of the United States of America, 107(49): 21046–21051

Feng X, Zhao C, D’Andrea W J, Hou J, Yang X, Xiao X, Shen J, Duan Y, Chen F (2022). Evidence for a relatively warm mid- to late Holocene on the southeastern Tibetan Plateau. Geophys Res Lett, 49(15): e2022GL098740

Feng X, Zhao C, D’Andrea W J, Liang J, Zhou A, Shen J (2019). Temperature fluctuations during the Common Era in subtropical southwestern China inferred from brGDGTs in a remote alpine lake. Earth Planet Sci Lett, 510: 26–36

Foster L C, Pearson E J, Juggins S, Hodgson D A, Saunders K M, Verleyen E, Roberts S J (2016). Development of a regional glycerol dialkyl glycerol tetraether (GDGT)–temperature calibration for Antarctic and sub-Antarctic lakes. Earth Planet Sci Lett, 433: 370–379

Günther F, Thiele A, Gleixner G, Xu B, Yao T, Schouten S (2014). Distribution of bacterial and archaeal ether lipids in soils and surface sediments of Tibetan lakes: implications for GDGT-based proxies in saline high mountain lakes. Org Geochem, 67: 19–30

He Y, Hou J, Wang M, Li X, Liang X, Xie S, Jin Y (2020). Temperature variation on the central Tibetan Plateau revealed by glycerol dialkyl glycerol tetraethers from the sediment record of Lake Linggo Co since the last deglaciation. Front Earth Sci (Lausanne), 8: 574206

Hou J, D'Andrea W J, Liu Z (2012). The influence of ^{14}C reservoir age on interpretation of paleolimnological records from the Tibetan Plateau. Quat Sci Rev, 48: 67–79

Hou J, Huang Y, Zhao J, Liu Z, Colman S, An Z (2016). Large Holocene summer temperature oscillations and impact on the peopling of the northeastern Tibetan Plateau. Geophys Res Lett, 43(3): 1323–1330

Hou J, Li C G, Lee S (2019a). The temperature record of the Holocene: progress and controversies. Sci Bull (Beijing), 64(9): 565–566

Hou S, Zhang W, Pang H, Wu S Y, Jenk T M, Schwikowski M, Wang Y (2019b). Apparent discrepancy of Tibetan ice core $\delta^{18}O$ records may be attributed to misinterpretation of chronology. Cryosphere, 13(6): 1743–1752

Immerzeel W W, van Beek L P H, Bierkens M F P (2010). Climate change will affect the Asian water towers. Science, 328(5984): 1382–1385

IPCC (2013). IPCC, 2013: Climate change 2013: the physical science basis. In: Contribution of Working Group I to the Fifth Assessment Report of the Intergovernmental Panel on Climate Change. Comput Geom, 18: 95–123

Jacob T, Wahr J, Pfeffer W T, Swenson S (2012). Recent contributions of glaciers and ice caps to sea level rise. Nature, 482(7386): 514–518

Kathayat G, Cheng H, Sinha A, Yi L, Li X, Zhang H, Li H, Ning Y, Edwards R L (2017). The Indian monsoon variability and civilization changes in the Indian subcontinent. Sci Adv, 3(12): e1701296

Kennett D J, Breitenbach S F, Aquino V V, Asmerom Y, Awe J, Baldini J U, Bartlein P, Culleton B J, Ebert C, Jazwa C, Macri M J, Marwan N, Polyak V, Prufer K M, Ridley H E, Sodemann H, Winterhalder B, Haug G H (2012). Development and disintegration of Maya political systems in response to climate change. Science, 338(6108): 788–791

Lei Y, Yang H, Dang X, Zhao S, Xie S (2016). Absence of a significant bias towards summer temperature in branched tetraether-based paleothermometer at two soil sites with contrasting temperature seasonality. Org Geochem, 94: 83–94

Li C G, Wang M, Liu W, Lee S Y, Chen F, Hou J (2021b). Quantitative estimates of Holocene glacier meltwater variations on the Western Tibetan Plateau. Earth Planet Sci Lett, 559: 116766

Li X, Fan B (2019). Climatic changes during the past 2000 years based on lake biomarkers from the central and western Tibetan Plateau. J Xinyang Normal Univ (Nat Sci Ed), 32(2): 239–244

Li X, Liu S, Fan B, Hou J, Wang M (2023b). Validating the potential application of δ^2H_{wax} and soil brGDGTs in paleoelevation estimates on the southern slopes of the Himalaya. Quat Sci Rev, 318: 108306

Li X, Liu S, Zhang L, Yan J, Fan B (2023a). Spatio-temporal patterns of centennial scale temperature change over the Tibetan Plateau during the past two millennia. J Xinyang Normal Univ (Nat Sci Ed), 36(3): 451–456

Li, X., Liu, S., Ji, K., Hou, X., Yuan, K., Hou, J., Niu, J., Yan, J., Yan, W., Wang, Y., Wang, Y., 2023. Late Holocene human population change revealed by fecal stanol records and its response to environmental evolution at Xiada Co on the western Tibetan Plateau. Palaeogeography, Palaeoclimatology, Palaeoecology, 111993.

Li X, Wang M, Hou J (2019). Centennial-scale climate variability during the past 2000 years derived from lacustrine sediment on the western Tibetan Plateau. Quat Int, 510: 65–75

Li X, Wang M, Zhang Y, Lei L, Hou J (2017). Holocene climatic and environmental change on the western Tibetan Plateau revealed by glycerol dialkyl glycerol tetraethers and leaf wax deuterium-to-hydrogen ratios at Aweng Co. Quat Res, 87(3): 455–467

Li X, Yan H, Fan B, Zhang C, Xing W (2021a). Climatic changes during the last two millennia on the southern Tibetan Plateau based on lake sediment and its forcing mechanisms. J Xinyang Normal Univ (Nat Sci Ed), 34(4): 584–588

Li X, Zhang X, Wu J, Shen Z, Zhang Y, Xu X, Fan Y, Zhao Y, Yan W (2011). Root biomass distribution in alpine ecosystems of the northern Tibetan Plateau. Environ Earth Sci, 64(7): 1911–1919

Liang J, Guo Y, Richter N, Xie H, Vachula R S, Lupien R L, Zhao B, Wang M, Yao Y, Hou J, Liu J, Russell J M (2022). Calibration and application of branched GDGTs to Tibetan lake sediments: the influence of temperature on the fall of the Guge Kingdom in Western Tibet, China. Paleoceanogr Paleoclimatol, 37(5)

Liu Z, Zhu J, Rosenthal Y, Zhang X, Otto-Bliesner B L, Timmermann A, Smith R S, Lohmann G, Zheng W, Elison Timm O (2014). The Holocene temperature conundrum. Proc Natl Acad Sci USA, 111(34): E3501–E3505

Marcott S A, Shakun J D, Clark P U, Mix A C (2013). A reconstruction of regional and global temperature for the past 11300 years. Science, 339(6124): 1198–1201

Mountain Research Initiative EDW Working Group (2015). Elevation-dependent warming in mountain regions of the world. Nature Climate Change, 5: 424–430

Naafs B D A, Inglis G N, Zheng C, Amesbury M J, Biester H, Bindler R, Blewett J, Burrows M A, del Castillo Torres D, Chambers F M, Cohen A D, Evershed R P, Feakins S J, Gałka M, Gallego-Sala A, Gandois L, Gray D M, Hatcher P G, Honorio Coronado E N, Hughes P D M, Huguet A, Könönen M, Laggoun-Défarge F, Lähteenoja O, Lamentowicz M, Marchant R, McClymont E, Pontevedra-Pombal X, Ponton C, Pourmand A, Rizzuti A M, Rochefort L, Schellekens J, De Vleeschouwer F, Pancost R D (2017). Introducing global peat-specific temperature and pH calibrations based on brGDGT bacterial lipids. Geochim Cosmochim Acta, 208: 285–301

Naeher S, Peterse F, Smittenberg R H, Niemann H, Zigah P K, Schubert C J (2014). Sources of glycerol dialkyl glycerol tetraethers (GDGTs) in catchment soils, water column and sediments of Lake Rotsee (Switzerland) – implications for the application of GDGT-based proxies for lakes. Org Geochem, 66: 164–173

Pang H, Hou S, Zhang W, Wu S, Jenk T M, Schwikowski M, Jouzel J (2020). Temperature trends in the northwestern Tibetan Plateau constrained by ice core water isotopes over the past 7000 years. J Geophys Res Atmos, 125(19)

Peterse F, van der Meer J, Schouten S, Weijers J W H, Fierer N, Jackson R B, Kim J H, Sinninghe Damsté J S (2012). Revised calibration of the MBT–CBT paleotemperature proxy based on branched tetraether membrane lipids in surface soils. Geochim Cosmochim Acta, 96: 215–229

Qian S, Yang H, Dong C, Wang Y, Wu J, Pei H, Dang X, Lu J, Zhao S, Xie S (2019). Rapid response of fossil tetraether lipids in lake sediments to seasonal environmental variables in a shallow lake in central China: implications for the use of tetraether-based proxies. Org Geochem, 128: 108–121

Russell J M, Hopmans E C, Loomis S E, Liang J, Sinninghe Damsté J S (2018). Distributions of 5- and 6-methyl branched glycerol dialkyl glycerol tetraethers (brGDGTs) in East African lake sediment: effects of temperature, pH, and new lacustrine paleotemperature calibrations. Org Geochem, 117: 56–69

Schouten S, Hopmans E C, Sinninghe Damsté J S (2013). The organic geochemistry of glycerol dialkyl glycerol tetraether lipids: a review. Org Geochem, 54: 19–61

Shanahan T M, Hughen K A, Van Mooy B A S (2013). Temperature sensitivity of branched and isoprenoid GDGTs in Arctic lakes. Org Geochem, 64: 119–128

Sinninghe Damsté J S (2016). Spatial heterogeneity of sources of branched tetraethers in shelf systems: the geochemistry of tetraethers in the Berau River delta (Kalimantan, Indonesia). Geochim Cosmochim Acta, 186: 13–31

Snyder C W (2010). The value of paleoclimate research in our changing climate. Clim Change, 100(3–4): 407–418

Sun Q, Chu G, Liu M, Xie M, Li S, Ling Y, Wang X, Shi L, Jia G, Lü H (2011). Distributions and temperature dependence of branched glycerol dialkyl glycerol tetraethers in recent lacustrine sediments from China and Nepal. J Geophys Res, 116: G01008

Sun Z, Hou X, Ji K, Yuan K, Li C, Wang M, Hou J (2022). Potential winter-season bias of annual temperature variations in monsoonal Tibetan Plateau since the last deglaciation. Quat Sci Rev, 292: 107690

Thompson L G, Mosley-Thompson E, Brecher H, Davis M, León B, Les D, Lin P N, Mashiotta T, Mountain K (2006). Abrupt tropical climate change: past and present. Proc Natl Acad Sci USA, 103(28): 10536–10543

Thompson L G, Yao T, Davis M, Henderson K, Mosley-Thompson E, Lin P N, Beer J, Synal H A, Cole-Dai J, Bolzan J (1997). Tropical climate instability: the last glacial cycle from a Qinghai-Tibetan ice core. Science, 276(5320): 1821–1825

Tierney J E, Russell J M, Eggermont H, Hopmans E, Verschuren D, Sinninghe Damsté J S (2010). Environmental controls on branched tetraether lipid distributions in tropical East African lake sediments. Geochim Cosmochim Acta, 74(17): 4902–4918

Wang H, Dong H, Zhang C L, Jiang H, Liu Z, Zhao M, Liu W (2015a). Deglacial and Holocene archaeal lipid-inferred paleohydrology and paleotemperature history of Lake Qinghai, northeastern Qinghai–Tibetan Plateau. Quat Res, 83(1): 116–126

Wang M D, Liang J, Hou J Z, Hu L (2016). Distribution of GDGTs in lake surface sediments on the Tibetan Plateau and its influencing factors. Sci China Earth Sci, 59(5): 961–974

Wang M, Hou J, Duan Y, Chen J, Li X, He Y, Lee S Y, Chen F (2021). Internal feedbacks forced Middle Holocene cooling on the Qinghai Tibetan Plateau. Boreas, 50(4): 1116–1130

Wang Z, Liu Z, Zhang F, Fu M, An Z (2015b). A new approach for reconstructing Holocene temperatures from a multi-species long chain alkenone record from Lake Qinghai on the northeastern Tibetan Plateau. Org Geochem, 88: 50–58

Wang Z, Zhang F, Cao Y, Hu J, Wang H, Lu H, Dong J, Xing M, Liu H, Wang H, Liu H (2022). Linking sedimentary and speleothem precipitation isotope proxy records to improve lacustrine and marine ^{14}C chronologies. Quat Sci Rev, 282: 107444

Weijers J W H, Bernhardt B, Peterse F, Werne J P, Dungait J A J, Schouten S, Sinninghe Damsté J S (2011). Absence of seasonal patterns in MBT–CBT indices in mid-latitude soils. Geochim Cosmochim Acta, 75(11): 3179–3190

Weijers J W H, Schouten S, Spaargaren O C, Sinninghe Damsté J S (2006). Occurrence and distribution of tetraether membrane lipids in soils: implications for the use of the TEX 86 proxy and the BIT index. Org Geochem, 37(12): 1680–1693

Weijers J W H, Schouten S, van den Donker J C, Hopmans E C, Sinninghe Damsté J S (2007). Environmental controls on bacterial tetraether membrane lipid distribution in soils. Geochim Cosmochim Acta, 71(3): 703–713

Wu D, Cao J, Jia G, Guo H, Shi F, Zhang X, Rao Z (2020). Peat brGDGTs-based Holocene temperature history of the Altai Mountains in arid Central Asia. Palaeogeogr Palaeoclimatol Palaeoecol, 538: 109464

Wu X, Dong H, Zhang C L, Liu X, Hou W, Zhang J, Jiang H (2013). Evaluation of glycerol dialkyl glycerol tetraether proxies for reconstruction of the paleo-environment on the Qinghai-Tibetan Plateau. Org Geochem, 61: 45–56

Yan T, Zhao C, Yan H, Shi G, Sun X, Zhang C, Feng X, Leng C (2021). Elevational differences in Holocene thermal maximum revealed by quantitative temperature reconstructions at ~30° N on eastern Tibetan Plateau. Palaeogeogr Palaeoclimatol Palaeoecol, 570: 110364

Yancheva G, Nowaczyk N R, Mingram J, Dulski P, Schettler G, Negendank J F, Liu J, Sigman D M, Peterson L C, Haug G H (2007). Influence of the intertropical convergence zone on the East Asian monsoon. Nature, 445(7123): 74–77

Yang H, Lü X, Ding W, Lei Y, Dang X, Xie S (2015). The 6-methyl branched tetraethers significantly affect the performance of the methylation index (MBT′) in soils from an altitudinal transect at Mount Shennongjia. Org Geochem, 82: 42–53

Yao T, Thompson L, Yang W, Yu W, Gao Y, Guo X, Yang X, Duan K, Zhao H, Xu B, Pu J, Lu A, Xiang Y, Kattel D B, Joswiak D (2012). Different glacier status with atmospheric circulations in Tibetan Plateau and surroundings. Nat Clim Chang, 2(9): 663–667

Yao T, Xue Y, Chen D, Chen F, Thompson L, Cui P, Koike T, Lau K M, Lettenmaier D, Mosbrugger V, Zhang R, Xu B, Dozier J, Gillespie T, Gu Y, Kang S, Piao S, Sugimoto S, Ueno K, Wang L, Wang W, Zhang F, Sheng Y, Guo W, Ailikun, Yang X, Ma Y, Shen S S P, Su Z, Chen F, Liang S, Liu Y, Singh V P, Yang K, Yang D, Zhao X, Qian Y, Zhang Y, Li Q (2019). Recent Third Pole's rapid warming accompanies cryospheric melt and water cycle intensification and interactions between monsoon and environment:

multi-disciplinary approach with observation, modeling and analysis. Bull Am Meteorol Soc, 100(3): 423–444

Zhang C, Zhao C, Yu S Y, Yang X, Cheng J, Zhang X, Xue B, Shen J, Chen F (2022). Seasonal imprint of Holocene temperature reconstruction on the Tibetan Plateau. Earth Sci Rev, 226: 103927

Zhang E, Chang J, Cao Y, Sun W, Shulmeister J, Tang H, Langdon P G, Yang X, Shen J (2017). Holocene high-resolution quantitative summer temperature reconstruction based on subfossil chironomids from the southeast margin of the Qinghai-Tibetan Plateau. Quat Sci Rev, 165: 1–12

Zhang Z, Tian H, Cazelles B, Kausrud K L, Bräuning A, Guo F, Stenseth N C (2010). Periodic climate cooling enhanced natural disasters and wars in China during AD 10-1900. Proc Biol Sci, 277(1701): 3745–3753

Zhao C, Rohling E J, Liu Z, Yang X, Zhang E, Cheng J, Liu Z, An Z, Yang X, Feng X, Sun X, Zhang C, Yan T, Long H, Yan H, Yu Z, Liu W, Yu S Y, Shen J (2021). Possible obliquity-forced warmth in southern Asia during the last glacial stage. Sci Bull (Beijing), 66(11): 1136–1145

Zhou W, Cheng P, Jull A, Lu X, An Z, Wang H, Zhu Y, Wu Z (2014). ^{14}C chronostratigraphy for Qinghai Lake in China. Radiocarbon, 56: 143–155

Zhu Z, Wu J, Rioual P, Mingram J, Yang H, Zhang B, Chu G, Liu J (2021). Evaluation of the sources and seasonal production of brGDGTs in lake Sihailongwan (N.E. China) and application to reconstruct paleo-temperatures over the period 60–8 ka BP. Quat Sci Rev, 261: 106946